β-Hydrogen-Containing Zirconium Alkyls with the Doubly-Bridged Bis(dimethylsilanediyl)dicyclopentadienyl Ligand. X-ray Molecular Structures of [Zr{$(SiMe_2)_2(\eta^5\text{-}C_5H_3)_2$}ClEt] and [Zr{$(SiMe_2)_2(\eta^5\text{-}C_5H_3)_2$}Et]$_2(\mu\text{-}CH_2{=}CH_2)$

Francisco J. Fernández,[†] Pilar Gómez-Sal,[†] Antonio Manzanero,[†] Pascual Royo,*[,†] Heiko Jacobsen,[‡] and Heinz Berke[‡]

Departamento de Química Inorgánica, Facultad de Ciencias, Universidad de Alcalá de Henares, 28871-Alcalá de Henares, Spain, and Anorganisch Chemisches Institut der Universität Zürich, Winterthurerstrasse 190, CH-8057 Zürich, Switzerland

Received December 12, 1996[⊗]

Alkylation of [Zr($CpSi_2Cp$)Cl_2] ($CpSi_2Cp$ = $(\eta^5\text{-}C_5H_3)_2[Si(CH_3)_2]_2$ with 1 equiv of RMgCl in THF at 10 °C gave the monoalkylated complexes [Zr($CpSi_2Cp$)ClR] (R = Et, n-Pr, *i*-Pr) in 80% yield, the isopropyl complex isomerizing to the *n*-propyl derivative above 10 °C. Addition of a second equivalent or an excess amount of the akylating agent resulted in the formation of the dialkyl compounds [Zr($CpSi_2Cp$)R_2] (R = Et, n-Pr). Hydrolysis of [Zr($CpSi_2Cp$)ClR] led to the μ-oxo dinuclear complex [{Zr($CpSi_2Cp$)Cl}$_2$(μ-O)]. Thermal decomposition of THF solutions of [Zr($CpSi_2Cp$)ClR] takes place with the evolution of an equimolar amount of alkane and alkene and the formation of [Zr($CpSi_2Cp$)Cl_2] and an unidentified residue. Formation of [Zr($CpSi_2Cp$)Et_2] is always accompanied by decomposition with the evolution of ethane to give [{Zr($CpSi_2Cp$)Et}$_2$(μ-$CH_2{=}CH_2$)] in 70% yield. A similar behavior was observed for [Zr($CpSi_2Cp$)(n-Pr)$_2$]. All of the compounds were characterized by elemental analysis and NMR spectroscopy, and the molecular structures of [Zr($CpSi_2Cp$)ClEt] and [{Zr($CpSi_2Cp$)-Et}$_2$(μ-$CH_2{=}CH_2$)] were studied by X-ray diffraction methods. Density functional calculations on the model compound [{$ZrCp_2Me$}$_2$(μ-$CH_2{=}CH_2$)] satisfactorily reproduce d_{C-C} = 1.482, $d1_{Zr-C}$ = 2.327 Å, and $d2_{Zr-C}$ = 2.506 Å, the geometry found experimentally.

Introduction

Numerous chemical and spectroscopic studies support the previously postulated metallocene cationic species[1] as the active intermediate for the chain-propagation step of metallocene-based catalysts for polymerization of α-olefins. Here, the coordination of the olefin at the vacant position is followed by insertion, with migration of the alkyl chain, leaving an alternating vacant site. Chain termination takes place by a dominant β-H elimination process,[2] which liberates the polymer with a terminal vinyl group. This results in a very reactive metal hydride intermediate that regenerates the starting active metallocene alkyl cation. Many efforts[3] have been made to discover the nature, structure, and reactivity of these intermediate metal−alkyl and metal−olefin species, but rather few alkyl compounds have been reported with β-H-containing functionalities.

Several examples of olefin-coordinated group 4 low-valent metal complexes of the type [MCp_2(olefin)L] have been reported.[4] These compounds usually contain additional phosphine ligands and form reasonably stable 18-electron compounds. To date, [$TiCp^*_2(CH_2{=}CH_2)$] is the unique ligand-free complex known of this type.[5] Even less is known about olefin-bridged dinuclear metal complexes,[6] and only [($ZrCp_2Me$)$_2$(μ-$CH_2{=}CH_2$)] has been structurally characterized by X-ray diffraction methods.[7]

Group 4 transition-metal−ethyl complexes have been isolated[8] by reaction of the olefin compounds [MCp_2-(olefin)L] with protonating electrophiles HX (X = halide,

[†] Universidad de Alcalá de Henares.
[‡] Anorganisch Chemisches Institut der Universität Zürich.
[⊗] Abstract published in *Advance ACS Abstracts,* March 1, 1997.

(1) (a) Eisch, J. J.; Piotrowski, A. M.; Brownstein, S. K.; Gabe, E. J.; Lee, F. L. *J. Am. Chem. Soc.* **1985**, *107*, 7219. (b) Jordan, R. F.; Bajgur, C. S.; Willet, R.; Scott, B. *J. Am. Chem. Soc.* **1986**, *108*, 7410. (c) Jordan, R. F.; Bradley, P. K.; Baenziger, N. C.; LaPointe, R. E. *J. Am. Chem. Soc.* **1990**, *112*, 1289. (d) Bochman, M.; Lancaster, S. J. *Organometallics* **1993**, *12*, 633. (e) Yang, X.; Stern, C. L.; Marks, T. J. *J. Am. Chem. Soc.* **1991**, *113*, 3623. (f) Brintzinger, H. H.; Fischer, D.; Mülhaupt, R.; Rieger, B; Waymouth, R. M. *Angew. Chem., Int. Ed. Engl.* **1995**, *34*, 1143.

(2) Tsutsui, T.; Mizuno, A.; Kashiwa, N. *Polymer* **1989**, *30*, 428.

(3) (a) Cohen, S. A.; Bercaw, J. E. *Organometallics* **1985**, *4*, 1006. (b) Negishi, E.; Swanson, D. R.; Miller, S. R. *Tetrahedron Lett.* **1988**, *29*, 1631. (c) Swanson, D. R.; Rousset, C. J.; Negishi, E.; Takahashi, T.; Seki, T.; Saburi, M.; Uchida, Y. *J. Org. Chem.* **1989**, *54*, 3521. (d) Takahashi, T.; Suzuki, N.; Kageyama, M.; Nitto, Y.; Saburi, M.; Negishi, E. *Chem. Lett.* **1991**, 1579. (e) Negishi, E.; Nguyen, T; Maye, J. P.; Choueiri, D.; Suzuki, N.; Takahashi, T. *Chem. Lett.* **1992**, 2367. (f) Takahashi, T.; Aoyagi, K.; Denisov, V.; Suzuki, N.; Choueiry, D.; Negishi, E. *Tetrahedron Lett.* **1993**, *34*, 8301.

(4) (a) Buchwald, S. L.; Watson, B. T. *J. Am. Chem. Soc.* **1986**, *108*, 7411. (b) Takahashi, T.; Swanson, D. R.; Negishi, E. *Chem. Lett.* **1987**, 623. (c) Alt, H. G.; Denner, C. E.; Thewalt, U.; Rausch, M. *J. Organomet. Chem.* **1988**, *356*, C83. (d) Takahashi, T.; Tamura, M.; Saburi, M.; Uchida, Y.; Negishi, E. *J. Chem. Soc., Chem. Commun.* **1989**, 852. (e) Takahashi, T.; Murakami, M.; Kunishige, M.; Saburi, M.; Uchida, Y.; Kozawa, K.; Uchida, T.; Swanson, D. R.; Negishi, E. *Chem. Lett.* **1989**, 761. (f) van Wagenen, B. C.; Livinghouse, T. *Tetrahedron Lett.* **1989**, *30*, 3495. (g) Takahashi, T.; Nitto, Y.; Seki, T.; Saburi, M.; Negishi, E. *Chem. Lett.* **1990**, 2259. (h) Fisher, R. A.; Buchwald, S. L. *Organometallics* **1990**, *9*, 871.

(5) Cohen, S. A.; Auburn, P. R.; Bercaw, J. E. *J. Am. Chem. Soc.* **1983**, *105*, 1136.

(6) Erker, G.; Kropp, K.; Atwood, J. L.; Hunter, W. E. *Organometallics* **1983**, *2*, 1555.

(7) Takahashi, T.; Kasai, K.; Suzuki, N.; Nakajima, K.; Negishi, E. *Organometallics* **1994**, *13*, 3413.

(8) Alt, H. G.; Denner, C. E. *J. Organomet. Chem.* **1990**, *391*, 53.

S0276-7333(96)01050-3 CCC: $14.00

alkoxide). The β-H containing substituents in these chloro alkyl compounds are easily isomerized[9] through the activation of one of the β C−H bonds to give highly unstable and reactive hydride species, which in turn are immediately transformed into the new isomerized alkyl ligand.

Previously, we reported[10,11] some group 4 *ansa*-metallocene complexes with the di-*ansa*-bis(dimethylsilandiyl)dicyclopentadienyl dianion, $[(\eta^5\text{-}C_5H_3)_2\text{-}(Me_2Si)_2]^{2-}$. This ligand increases the stereorigidity of the complex and usually leads to rather close bending angles, θ, between the cyclopentadienyl rings when compared with typical values of 123−134°.[12] In the present paper, we report the isolation of β-H containing zirconocene alkyls and their thermal behavior leading to the first dinuclear ethyl μ-ethene zirconium complex, $[\{Zr(CpSi_2Cp)Et\}_2(\mu\text{-}CH_2{=}CH_2)]$. The X-ray molecular structure shows unusual features, which can be related to the extremely narrow bending angle of the zirconocene fragments. We also discuss the preparative, structural, and spectroscopic aspects of these compounds. Finally, we present calculations on the model compound $[\{ZrCp_2Et\}_2(\mu\text{-}CH_2{=}CH_2)]$ in order to analyze the bonding of the μ-ethene moiety in $[\{Zr(CpSi_2Cp)\text{-}Et\}_2(\mu\text{-}CH_2{=}CH_2)]$. These calculations are based on approximate density functional theory (DFT), which is now well-established as a valuable tool in studying the structures and energetics of transition metal compounds.[13]

Experimental Section

All operations were performed under an inert atmosphere of argon using Schlenk and vacuum-line techniques or a VAC glovebox, Model HE-63-P. The following solvents were dried and purified by distillation under argon before use by employing the appropriate drying/deoxygenating agents: tetrahydrofuran (THF, sodium/benzophenone), toluene (sodium), and hexane (sodium/potassium alloy). $[ZrCl_2\{(\eta^5\text{-}C_5H_3)_2[Si(CH_3)_2]_2\}]$ (**1**) was prepared according to literature procedures.[10] EtMgCl (Aldrich), (n-Pr)MgCl (Aldrich), (*i*-Pr)MgCl (Aldrich), and PMe_3 (Aldrich) were purchased from commercial sources and used without further purification. ^{1}H, ^{13}C, and $^{13}C\{^1H\}$ NMR spectra were recorded on Varian 300 Unity and Varian 500 Unity Plus instruments. ^{1}H and ^{13}C chemical shifts are reported in parts per million (ppm, δ, units positive chemical shifts to a higher frequency) relative to TMS. Mass spectra were recorded on a Hewlett Packard 5890 spectrometer. Elemental C and H analyses were performed with a Perkin-Elmer 240B microanalyzer.

Synthesis of $[ZrCl(CH_2\text{-}CH_3)\{(\eta^5\text{-}C_5H_3)_2[Si(CH_3)_2]_2\}]$, 2. 1.23 mL of a 2M THF solution of EtMgCl were added to a THF solution (25 mL) of $[ZrCl_2\{(\eta^5\text{-}C_5H_3)_2[Si(CH_3)_2]_2\}]$ **1** (1 g, 2.47 mmol) at −78 °C. The mixture was warmed at 10 °C and stirred for 12 h to give a red solution which after evaporation of the solvent and extraction with toluene rendered complex **2**, which was recrystallized from hexane as yellow crystals (0.79 g, 80%). Anal. Calcd for $C_{16}H_{23}Si_2ClZr$: C, 48.26; H, 5.82. Found: C, 48.04; H, 5.87. CIMS: $[M^+ - (CH_2{-}CH_3)]$ $m/e = 367$ (100); $[M^+]$ was not observed. ^{1}H NMR (300 MHz, C_6D_6): δ 6.71 (2H, m, C_5H_3), 6.55 (2H, m, C_5H_3), 6.28 (2H, m, C_5H_3), 1.53 (3H, t, $J = 7.7$ Hz, $-CH_2{-}CH_3$), 1.04 (2H, q, $J = 7.7$ Hz, $-CH_2{-}CH_3$), 0.50 (3H, s, $Si(CH_3)_2$), 0.43 (3H, s, $Si(CH_3)_2$), 0.31 (3H, s, $Si(CH_3)_2$), 0.01 (3H, s, $Si(CH_3)_2$). ^{1}H-NMR (500 MHz, THF-d_8): δ 6.81 (2H, m, C_5H_3), 6.70 (2H, m, C_5H_3), 6.41 (2H, m, C_5H_3), 1.26 (3H, t, $J = 8.0$ Hz, $-CH_2{-}CH_3$), 0.90 (2H, q, $J = 8.0$ Hz, $-CH_2{-}CH_3$), 0.80 (3H, s, $Si(CH_3)_2$), 0.74 (3H, s, $Si(CH_3)_2$), 0.50 (3H, s, $Si(CH_3)_2$), 0.37 (3H, s, $Si(CH_3)_2$). ^{13}C-NMR (75 MHz, C_6D_6): δ 134.0 (C_5H_3), 132.0 (C_5H_3), 116.4 (C_5H_3, ipso), 113.7 (C_5H_3), 110.1 (C_5H_3, ipso), 44.8 (t, $J_{CH} = 116.3$ Hz, $-CH_2{-}CH_3$), 18.0 (q, $J_{CH} = 124.5$ Hz, $-CH_2{-}CH_3$), 2.2 ($Si(CH_3)_2$), 2.1 ($Si(CH_3)_2$), −3.6 ($Si(CH_3)_2$), −5.2 ($Si(CH_3)_2$).

Synthesis of $[ZrCl(CH_2{-}CH_2{-}CH_3)\{(\eta^5\text{-}C_5H_3)_2[Si(CH_3)_2]_2\}]$, 3. A 2 M diethyl ether solution of (n-Pr)MgCl (1.23 mL) was added to a THF solution (25 mL) of $[ZrCl_2\{(\eta^5\text{-}C_5H_3)_2\text{-}[Si(CH_3)_2]_2\}]$, **1** (1 g, 2.47 mmol), at −78 °C. The mixture was warmed at 10 °C and stirred for 12 h to give a brown solution. The solvent was completely removed in vacuo, and the residue was extracted with toluene to render complex **3**, which was recrystallized from diethyl ether as yellow-brown crystals (0.712 g, 70% yield). Anal. Calcd for $C_{17}H_{25}Si_2ClZr$: C, 49.53; H, 6.11. Found: C, 49.79; H, 6.50. CIMS: $[M^+ - (CH_2{-}CH_2{-}CH_3)]$ $m/e = 367$ (100); $[M^+]$ was not observed. ^{1}H-NMR (300 MHz, C_6D_6): δ 6.70 (2H, m, C_5H_3), 6.58 (2H, m, C_5H_3), 6.27 (2H, m, C_5H_3), 1.75 (2H, m, $-CH_2{-}CH_2{-}CH_3$), 1.08 (3H, m, $-CH_2{-}CH_2{-}CH_3$), 1.04 (2H, m, $-CH_2{-}CH_2{-}CH_3$), 0.50 (3H, s, $Si(CH_3)_2$), 0.44 (3H, s, $Si(CH_3)_2$), 0.32 (3H, s, $Si(CH_3)_2$), 0.02 (3H, s, $Si(CH_3)_2$). ^{1}H-NMR (500 MHz, THF-d_8): δ 6.81 (2H, m, C_5H_3), 6.65 (2H, m, C_5H_3), 6.38 (2H, m, C_5H_3), 1.52 (2H, m, $-CH_2{-}CH_2{-}CH_3$), 0.88 (2H, m, $CH_2{-}CH_2{-}CH_3$), 0.77 (3H, s, $Si(CH_3)_2$), 0.70 (3H, s, $Si(CH_3)_2$), 0.47 (3H, s, $Si(CH_3)_2$), 0.34 (3H, s, $Si(CH_3)_2$). ^{13}C-NMR (75 MHz, C_6D_6): 134.4 (C_5H_3), 131.9 (C_5H_3), 116.2 (C_5H_3 ipso), 113.7 (C_5H_3), 110.0 (C_5H_3, ipso), 56.2 (t, $CH_2{-}CH_2{-}CH_3$ t, J_{CH} (125 MHz, THF-d_8) = 116.7 Hz), 27.5 (t, $-CH_2{-}CH_2{-}CH_3$, J_{CH} (125 MHz, THF-d_8) = 119.3 Hz), 20.8 (q, $-CH_2{-}CH_2{-}CH_3$, J_{CH} (125 MHz, THF-d_8) = 124.8 Hz), 2.25 ($Si(CH_3)_2$), 2.20 ($Si(CH_3)_2$), −3.6 ($Si(CH_3)_2$), −5.14 ($Si(CH_3)_2$).

Reaction of $[ZrCl_2\{(\eta^5\text{-}C_5H_3)_2[Si(CH_3)_2]_2\}]$, 1, with (*i*-Pr)MgCl. A 2 M diethyl ether solution of (*i*-Pr)MgCl (1.23 mL) was added to a THF solution (25 mL) of $[ZrCl_2\{(\eta^5\text{-}C_5H_3)_2\text{-}[Si(CH_3)_2]_2\}]$, **1** (1 g, 2.47 mmol), at −78 °C. The mixture was warmed to 10 °C and stirred for 12 h to give a brown solution. The solvent was removed in vacuo to give a yellow-brown solid, which was extracted with toluene. Recrystallization from diethyl ether gave a mixture of $[ZrCl(CH(CH_3)_2)\{(\eta^5\text{-}C_5H_3)_2\text{-}[Si(CH_3)_2]_2\}]$, **4**, and complex **3**, which was characterized by ^{1}H NMR spectroscopy. When the reaction was monitored by NMR spectroscopy in a sealed NMR tube using a mixture of compound **1** (0.04 g, 0.1 mmol) and a 2 M diethyl ether solution of (*i*-Pr)MgCl (0.05 mL, 0.1 mmol) in THF-d_8 (0.75 mL), pure isopropyl complex **4** was characterized by NMR spectroscopy as the unique organometallic compound in the solution after 1 h at 10 °C, although it was not isolated as a solid. ^{1}H-NMR (300 MHz, C_6D_6): δ 6.75 (2H, m, C_5H_3), 6.52 (2H, m, C_5H_3), 6.28 (2H, m, C_5H_3), 1.54 (6H, d, $J = 7.3$ Hz, $-CH{-}(CH_3)_2$), 0.50 (3H, s, $Si(CH_3)_2$), 0.45 (3H, s, $Si(CH_3)_2$), 0.34 (3H, s, $Si(CH_3)_2$), 0.04 (3H, s, $Si(CH_3)_2$). ^{1}H-NMR (500 MHz, THF-d_8): δ 6.76 (2H, m, C_5H_3), 6.69 (2H, m, C_5H_3), 6.40 (2H, m, C_5H_3), 1.33 (6H, d, $J = 8.0$ Hz, $-CH{-}(CH_3)_2$), 0.77 (3H, s, $Si(CH_3)_2$), 0.72 (3H, s, $Si(CH_3)_2$), 0.71 (1H, spt, $J = 8$ Hz, $-CH{-}(CH_3)_2$), 0.46 (3H, s, $Si(CH_3)_2$), 0.36 (3H, s, $Si(CH_3)_2$). ^{13}C-NMR (125 MHz, THF-d_8): δ 136.3 (C_5H_3), 131.8 (C_5H_3), 118.2 (C_5H_3 ipso), 116.1 (C_5H_3), 112.7 (C_5H_3, ipso), 57.9 ($-CH{-}(CH_3)_2$), 29.9 ($-CH{-}(CH_3)_2$), 3.7 ($Si(CH_3)_2$), 3.6 ($Si(CH_3)_2$), −2.4 ($Si(CH_3)_2$), −3.7 ($Si(CH_3)_2$).

Synthesis of $[\{ZrCl[(\eta^5\text{-}C_5H_3)_2[Si(CH_3)_2]_2]\}_2(\mu\text{-}O)]$, 5. A 1 M toluene solution of PMe_3 (2 mL, 2 mmol) and water (0.018 mL, 1 mmol) were added to a toluene solution (50 mL) of complex **3** (0.8 g, 1.9 mmol). The mixture was refluxed and stirred for 24 h to give a yellow solution, which was filtered,

(9) Swanson, D. R.; Negishi, E. *Organometallics* **1991**, *10*, 825.
(10) (a) Cano, A.; Cuenca, T.; Gómez-Sal, P.; Royo, B.; Royo, P. *Organometallics* **1994**, *13*, 1688. (b) Cano, A.; Gómez-Sal, P.; Manzanero, A.; Royo, P. *J. Organomet. Chem.* **1996**, *526*, 227.
(11) Cuenca, T.; Galakhov, M.; Royo, E.; Royo, P. *J. Organomet. Chem.* **1996**, *515*, 33.
(12) Höweler, U.; Mohr, R.; Knickmeier, M.; Erker G. *Organometallics* **1994**, *13*, 2380.
(13) (a) Ziegler, T. *Pure. Appl. Chem.* **1991**, *28*, 1271. (b) Ziegler, T. *Chem. Rev.* **1991**, *91*, 651. (c) Ziegler, T. *Can. J. Chem.* **1995**, *73*, 743.

Table 1. Crystal Data and Structure Refinement for Compounds 2 and 8

	compound **2**	compound **8**
cryst size	0.2 × 0.3 × 0.3	0.2 × 0.2 × 0.3
color	yellow-pale	yellow-pale
cryst habit	prismatic	prismatic
empirical formula	$ZrSi_2ClC_{16}H_{23}$	$Zr_2Si_4C_{34}H_{50}$
fw	398.21	753.54
temp	293(2) K	293(2) K
wavelength	0.710 69 Å	0.710 69 Å
cryst syst	monoclinic	monoclinic
space group	$P2_1$	$P2_1/n$
unit cell dimens	a = 9.204(3) Å b = 13.574(2) Å c = 14.758(6) Å β = 104.91(2)°	a = 8.715(3) Å b = 8.066(2) Å c = 25.125(5) Å β = 91.38(2)°
volume	1781(1) Å^3	1765.7(8) Å^3
Z	4	2
density(calcd)	1.485 g/cm^3	1.417 g/cm^3
abs coeff	8.80 cm^{-1}	7.48 cm^{-1}
F(000)	816	780
scan mode	$\omega/2\theta$ scans	$\omega/2\theta$ scans
θ range for data collection	2.00−30.00	2.00−27.00
index ranges	$0 < h < 12$, $0 < k < 19$, $-20 < l < 20$	$-11 < h < 11$, $0 < k < 10$, $0 < l < 32$
no. reflns collected	5572	4005
no. reflns obs with $I > 2\sigma(I)$	3353	2930
abs correction	N/A	N/A
refinement method	full-matrix least-squares on F	full-matrix least-squares on F^2
goodness-of-fit on F^2	1.164	0.994
final R indices [$I > 2\sigma(I)$]	R1 = 0.0330, wR2 = 0.0381	R1 = 0.0461, wR2 = 0.1280
weighting scheme	$w = 4F_o^2/[\sigma(F_o)^2]^2$	$w = 1/[\sigma^2(F_o^2) + (0.0870P)^2 + 4.5349P]$ where $P = (F_o^2 + 2F_c^2)/3$
largest diff peak and hole	0.425 and −0.524 e Å^{-3}	1.363 and −0.957 e Å^{-3}

concentrated to 5 mL, and cooled to −20 °C to provide white crystals of compound **5** (0.537 g, 75%). Anal. Calcd for $C_{28}H_{36}Si_4Cl_2Zr_2O$: C, 44.58; H, 4.81. Found: C, 44.59; H, 4.77. CIMS: [M$^+$] m/e = 754 (1); [M$^+$ − (CH$_3$)] m/e = 739 (21); [ZrCl{(η^5-C_5H_3)$_2$[Si(CH$_3$)$_2$]$_2$}]$^+$ m/e = 367 (10); [ZrO{(η^5-C_5H_3)$_2$[Si(CH$_3$)$_2$]$_2$}]$^+$ m/e = 351 (10). ^{1}H-NMR (300 MHz, C_6D_6): 6.97 (4H, m, C_5H_3), 6.96 (4H, m, C_5H_3), 6.26 (4H, m, C_5H_3), 0.71 (6H, s, Si(CH_3)$_2$), 0.61 (6H, s, Si(CH_3)$_2$), 0.56 (6H, s, Si(CH_3)$_2$), 0.39 (6H, s, Si(CH_3)$_2$). ^{13}C-NMR (75 MHz, C_6D_6): 138.3 (C_5H_3), 136.1 (C_5H_3), 120.4 (C_5H_3, ipso), 115.2 (C_5H_3, ipso), 112 (C_5H_3), 2.4 (Si(CH_3)$_2$), 1.8 (Si(CH_3)$_2$), −3.8 (Si(CH_3)$_2$), −4.5 (Si(CH_3)$_2$).

Reaction of [ZrCl$_2${(η^5-C_5H_3)$_2$[Si(CH$_3$)$_2$]$_2$}], 1, with an Excess Amount of EtMgCl. A mixture of **1** (0.5 g, 0.12 mmol) and a 2 M THF solution of EtMgCl (0.125 mL, 0.25 mmol) in THF-d_8 (0.75 mL) was sealed under vacuum in a NMR tube at −78 °C, and the reaction was monitored by ^{1}H and ^{13}C NMR spectroscopies. After 1 h at −10 °C, **1** had been totally transformed into complex **2**, and then resonances due to [Zr(CH$_2$-CH$_3$)$_2$ {(η^5-C_5H_3)$_2$[Si(CH$_3$)$_2$]$_2$}], **6**, appeared. After 1.5 h, this was the only organometallic complex present in the solution, together with the excess EtMgCl. When the temperature was raised to 20 °C, the resonances due to complex **6** disappeared, and new resonances due to its decomposition products were observed. Data for complex **6**: ^{1}H-NMR (500 MHz, THF-d_8, −10 °C) 6.51 (4H, d, C_5H_3), 6.38 (2H, t, C_5H_3), 1.07 (6H, t, J = 8.0 Hz, −CH$_2$−CH_3), 0.59 (6H, s, Si(CH_3)$_2$), 0.27 (6H, s, Si(CH_3)$_2$), 0.15 (4H, q, J = 8.0 Hz, −CH_2−CH$_3$). ^{13}C-NMR (125 MHz, THF-d_8, −30 °C): δ 129.4 (C_5H_3), 113.1 (C_5H_3), 111.2 (C_5H_3, ipso), 42.7 (−CH_2−CH$_3$), 16.6 (−CH$_2$−CH_3), 2.6 (Si(CH_3)$_2$), −4.2 (Si(CH_3)$_2$).

Reaction of [ZrCl$_2${(η^5-C_5H_3)$_2$[Si(CH$_3$)$_2$]$_2$}], 1, with an Excess Amount of (n-Pr)MgCl. A mixture of **1** (0.5 g, 0.12 mmol) and a 2 M diethyl ether solution of (n-Pr)MgCl (0.125 mL, 0.25 mmol) in 0.75 mL of THF-d_8 was sealed under vacuum in a NMR tube at −78 °C. The reaction was monitored by ^{1}H and ^{13}C NMR spectroscopies. After 1 h at −10 °C, all of **1** had been transformed into complex **3**, when resonances due to [Zr(CH$_2$−CH$_2$−CH$_3$)$_2$ {(η^5-C_5H_3)$_2$[Si(CH$_3$)$_2$]$_2$}] started to appear. After 1.5 h at −5 °C, **7** was the only organometallic complex present in the solution together with the excess (n-Pr)MgCl. When the temperature was raised to 20 °C, the resonances due to complex **7** disappeared and new resonances due to unidentified decomposition products were observed. ^{1}H-NMR (500 MHz, THF-d_8, −5 °C): δ 6.54 (4H, d, C_5H_3), 6.36 (2H, t, C_5H_3), 1.34 (4H, m, −CH$_2$−CH_2−CH$_3$), 0.7 (6H, m, −CH$_2$−CH$_2$−CH_3), 0.60 (6H, s, Si(CH_3)$_2$), 0.28 (6H, s, Si(CH_3)$_2$), 0.18 (4H, m, −CH_2−CH$_2$−CH$_3$). ^{13}C-NMR (125 MHz, THF-d_8, −5 °C): δ 130.6 (C_5H_3), 114.4 (C_5H_3), 112.4 (C_5H_3, ipso), 56.4 (−CH_2−CH$_2$−CH$_3$), 28.2 (−CH$_2$−CH_2−CH$_3$), 23.2 (−CH$_2$−CH$_2$−CH_3), 3.8 (Si(CH_3)$_2$), −2.9 (Si(CH_3)$_2$).

Synthesis of [{Zr(CH$_2$-CH$_3$)[(η^5-C_5H_3)$_2$[Si(CH$_3$)$_2$]$_2$]}$_2${μ-[η^2-(CH$_2$−CH$_2$)}], 8. A 2 M THF solution of EtMgCl (2.46 mL) was added to a THF solution of **1** (1 g, 2.47 mmol) at −78 °C. The mixture was warmed to 0 °C and stirred for 3 h to give a red solution, which after evaporation of the solvent and recrystallization from a mixture of diethyl ether−hexane (10/5) rendered orange crystals of complex **8** (0.651 g, 70%). CIMS: [M$^+$ − (CH$_2$−CH$_3$)] m/e = 723 (3.8), [M$^+$ − (CH$_2$CH$_3$) − (SiMe$_2$)] m/e = 665 (8.5), [Zr(CH$_2$−CH$_3$)[(η^5-C_5H_3)$_2$[Si(CH$_3$)$_2$]$_2$]$^+$ m/e = 360 (4.9), [Zr[(η^5-C_5H_3)$_2$[Si(CH$_3$)$_2$]$_2$]$^+$ m/e = 331(100). ^{1}H-NMR (300 MHz, C_6D_6): 6.44 (4H, m, C_5H_3), 6.36 (4H, m, C_5H_3), 5.41 (4H, m, C_5H_3), 1.60 (6H, t, J = 7.7 Hz, −CH$_2$−CH_3), 0.82 (4H, q, J = 7.7 Hz, −CH_2−CH$_3$), 0.65 (6H, s, Si(CH_3)$_2$), 0.64 (6H, s, Si(CH_3)$_2$), 0.53 (6H, s, Si(CH_3)$_2$), 0.43 (6H, s, Si(CH_3)$_2$), −0.10 (4H, s, [η^2(−CH_2−CH_2−)]. ^{13}C-NMR (75 MHz, C_6D_6): δ 131.0 (C_5H_3), 127.3 (C_5H_3), 108.1 (C_5H_3, ipso), 105 (C_5H_3), 104.7 (C_5H_3, ipso), 22.7 (−CH_2−CH$_3$), 20.7 (q, J_{CH} = 122.2 Hz, −CH$_2$−CH_3), δ 9.0 (t, J_{CH} = 141 Hz, [η^2-(−CH_2−CH_2−)], 3.7 (Si(CH_3)$_2$), 3.4 (Si(CH_3)$_2$), −3.4 (Si(CH_3)$_2$), −3.9 (Si(CH_3)$_2$).

Crystal Structure Determination of Compounds 2 and 8. Crystallographic and experimental details of the crystal structure determinations are given in Table 1. Suitable crystals of complexes **2** and **8** were mounted on an Enraf-Nonius CAD 4 automatic four-circle diffractometer with bisecting geometry, equipped with a graphite-oriented monochromator and Mo Kα radiation (λ = 0.710 69 Å). Data were collected at room temperature. Intensities were corrected for Lorentz and polarization effects in the usual manner. No absorption or extinction corrections were made.

The structure of **2** was solved by a combination of direct methods and Fourier synthesis and refined (on F) by full-matrix least-squares calculations using the SDP[14] package. All of the non-hydrogen atoms were refined anisotropically. In

the last cycle of the refinement, the hydrogen atoms were introduced from geometric calculations, refined one cycle isotropically, and then fixed, except for the hydrogen atoms bonded to C(1) and C(2), which were found in the difference Fourier map and then fixed in their positions. Final values of $R = 0.0330$ and $R_w = 0.0381$ were obtained for **2**.

The structure of **8** was solved by direct methods (SHELXS 90)[15] and refined by full-matrix least-squares against F^2 (SHELXL 93).[16] All of the non-hydrogen atoms were refined anisotropically. In the last cycle of refinement, the hydrogen atoms were positioned geometrically and refined using a riding model with fixed thermal parameters, except for the hydrogen atoms bonded to C(31) and C(41), which were located in the difference Fourier map and then refined.

Calculations were carried out on an ALPHA AXP (Digital) workstation.

Computational Details. All calculations are based on the local density approximation (LDA) in the parametrization of Vosko, Wilk, and Nussair.[17] Nonlocal gradient corrections due to exchange[18] and correlation[19] were included self-consistently (NL-SCF). The calculations utilized the Amsterdam Density Functional (ADF) package,[20] release 2.0.1. Use was made of the frozen core approximation. For C, the valence shells were described using a double ζ-STO (Slater-type orbital) basis, augmented by one *d*-STO polarization function (ADF database III). For the *n*s, *n*p, *n*d, $(n + 1)$s, and $(n + 1)$p shells on Zr, a triple ζ-STO basis was employed (ADF database IV, augmented by $\alpha_{5p} = 0.85$, 1.30, and 2.05). H was treated with a double ζ-STO basis and one additional *p*-STO polarization function (ADF database III). The numerical integration grid was chosen so that significant test integrals were evaluated with an accuracy of at least four significant digits. In geometry optimizations, the arrangements of the cyclopentadienyl and methyl ligands were fixed, based on the geometry of [{Zr($CpSi_2$-Cp)Et}$_2$(μ-CH_2=CH_2)] in the solid state.

Results and Discussion

Chloro Alkyl Complexes. Previously, we reported[10a] the isolation of the di-*ansa*-zirconocene dichloride [Zr($CpSi_2Cp$)Cl_2] (**1**, $CpSi_2Cp$ = 1,1′,2,2′-$(SiMe_2)_2(\eta^5$-$C_5H_3)_2$) from $ZrCl_4$ and the dilithium salt of the ligand.

Complex **1** reacts with a THF solution of 1 equiv of RMgCl (R = Et, n-Pr) providing the chloro alkyl complexes [Zr($CpSi_2Cp$)ClR] (R = Et (**2**), n-Pr (**3**)), which were isolated as yellow (**2**) or yellow-brown (**3**) crystals in 80% (from hexane) and 70% (from diethyl ether) yield, respectively (Scheme 1). The reaction is complete after stirring for 12 h at 10 °C. An excess amount of the alkylating agent must be avoided to prevent the formation of the dialkyl compound, and the temperature must not exceed 15 °C to prevent decomposition. ^{1}H and ^{13}C NMR data (see Experimental Section) as well as the elemental analysis for compounds **2** and **3** were consistent with their proposed structures; the molecular structure of **2** was subsequently confirmed by X-ray diffraction and is shown in Figure 1, with the atomic labeling scheme. Selected bond distances and angles are given in Table 2.

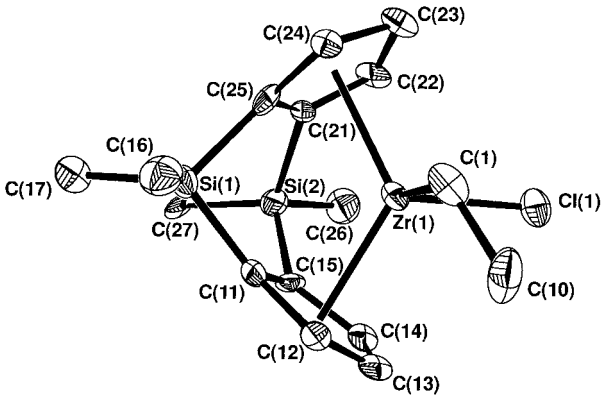

Figure 1. ORTEP view of the molecular structure of [Zr($CpSi_2Cp$)ClEt] (**2**), with the atom numbering scheme.

Scheme 1

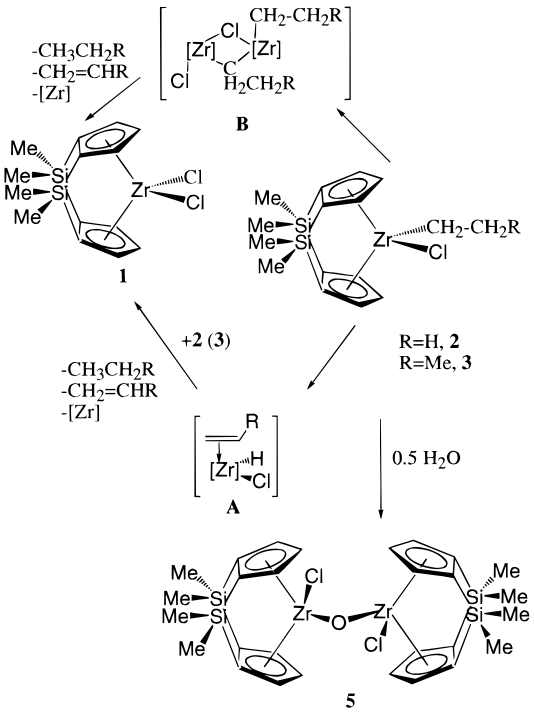

In the asymmetric unit of the unit cell, two different conformations of compound **2** exist, which only differ in the orientation of the ethyl system. The data belonging to the second molecule are included in brackets. The molecule can be described as a pseudo-tetrahedral zirconium complex, if both cyclopentadienyl ring centroids are considered as single coordination sites. The chlorine and the ethyl C_α atoms together with the Zr atom define the equatorial plane. The bond distances to the metal center ($d_{Zr-Cl} = 2.436(2)$ [2.440(2)] Å and $d_{Zr-C\alpha} = 2.249(7)$ [2.277(6)] Å) correspond to single bonds. Both cyclopentadienyl rings are eclipsed, and the centroid to Zr distances range from 2.209 to 2.218 Å. The zirconium atom penetrates the metallocene wedge, which may result from polarization of the Cp ligands due to the presence of the two electron withdrawing silyl groups. The metal center is located at distances from the internal bridgehead carbon atoms about 0.1 Å shorter than those from the external ones, which leads to significant differences in the electronic properties of the ring carbon atoms. The bending angle θ between the two cyclopentadienyl rings is 120.6° [120.2°], which is comparable to that found for [Zr($CpSi_2$-

(14) B. A. Frenz, and Associates, Inc. SDP; Texas A & M and Enraf-Nonius, College Station, TX 77840, Delft, Holland, 1985.
(15) Sheldrick, G. M. *Acta Crystallogr., Sect. A* 1190, *46*, 467.
(16) Sheldrick, G. M. *SHELXL93*; University of Göttingen: Göttingen, Germany, 1993.
(17) Vosko, S. J.; Wilk, M.; Nussair, M. *Can. J. Phys.* **1980**, *58*, 1200.
(18) (a) Becke, A. *J. Chem. Phys.* **1988**, *88*, 1053. (b) Becke, A. *Phys. Rev.* **1988**, *A38*, 3098.
(19) (a) Perdew, J. P. *Phys. Rev.* **1986**, *B33*, 8822. (b) Perdew, J. P. *Phys. Rev.* **1986**, *B34*, 7406.
(20) (a) Baerends, E. J.; Ellis, D. E.; Ros, P. E. *Chem. Phys.* **1973**, *2*, 41. (b) teVelde, G.; Baerends, E. J. *J. Comput. Phys.* **1992**, *99*, 84.
(21) Jordan, R. F. *J. Organomet. Chem.* **1985**, *294*, 321.

Scheme 2

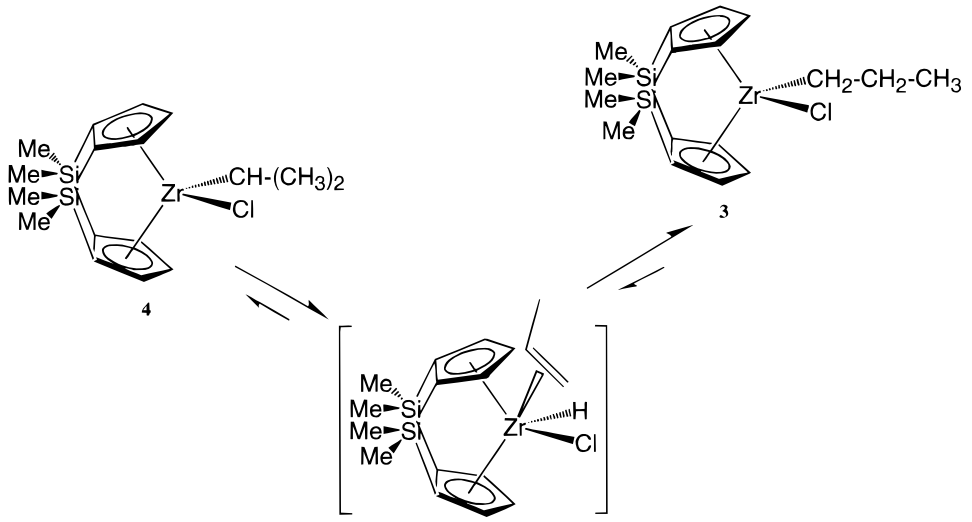

Table 2. Selected Bond Distances (Å) and Angles (deg) for Compound 2[a]

Zr−Cl2	2.436(2)	Zr2−C43	2.622(6)	C11−C15	1.429(8)
Zr1−C1	2.249(7)	Zr2−C44	2.535(5)	C12−C13	1.333(9)
Zr1−C11	2.443(5)	Zr2−C45	2.472(5)	C13−C14	1.297(8)
Zr1−C12	2.566(5)	Si1−C11	1.802(7)	C14−C15	1.452(9)
Zr1−C13	2.605(5)	Si1−C25	1.879(5)	C21−C22	1.271(8)
Zr1−C14	2.546(5)	Si1−C16	1.871(7)	C21−C25	1.467(8)
Zr1−C15	2.445(6)	Si1−C17	1.799(6)	C22−C23	1.459(9)
Zr1−C21	2.394(6)	Si2−C15	1.909(5)	C23−C24	1.536(8)
Zr1−C22	2.486(5)	Si2−C21	1.916(6)	C24−C25	1.355(8)
Zr1−C23	2.643(6)	Si2−C26	1.813(9)	C2−C20	1.577(8)
Zr1−C24	2.600(6)	Si2−C27	1.880(8)	C31−C32	1.479(8)
Zr1−C25	2.463(6)	Si3−C31	1.873(5)	C31−C35	1.448(8)
Zr2−Cl2	2.440(2)	Si3−C36	1.848(7)	C32−C33	1.272(7)
Zr2−C2	2.277(6)	Si3−C37	1.967(8)	C33−C34	1.373(9)
Zr2−C31	2.420(6)	Si3−C45	1.928(5)	C34−C35	1.536(8)
Zr2−C32	2.498(5)	Si4−C35	1.859(6)	C41−C42	1.37(1)
Zr2−C33	2.576(6)	Si4−C41	1.850(6)	C41−C45	1.480(7)
Zr2−C34	2.623(6)	Si4−C46	1.880(8)	C42−C43	1.527(9)
Zr2−C35	2.488(6)	Si4−C47	1.890(7)	C43−C44	1.514(9)
Zr2−C41	2.446(6)	C1−C10	1.48(1)	C44−C45	1.288(8)
Zr2−C42	2.541(7)	C11−C12	1.565(8)		

Cl1−Zr1−C1	96.1(2)	Cl2−Zr2−C2	99.9(2)
C10−C1−Zr1	114.6(5)	C20−C2−Zr2	118.6(4)
C25−Si1−C11	92.9(2)	C21−Si2−C15	92.0(3)
C31−Si3−C45	92.3(2)	C35−Si4−C41	93.2(2)

[a] Numbers in parentheses are estimated standard deviations in the least significant digits.

Cp)Cl_2][10] [120.6°] but narrower than the usual angle range from 123° to 134°.[12] The plane defined by the C_α, C_β, and Zr atoms is oriented toward one of the cyclopentadienyl rings, forming a dihedral angle of 63.0(4)° [63.1(4)°] with the equatorial plane. The Cβ atom of the ethyl group is located 1.143(8) [1.187(7)] Å out of the equatorial plane. Although this makes the two cyclopentadienyl rings chemically inequivalent, this cannot be detected in the solution NMR spectra at temperatures down to −80 °C. The observed positions of the two Cα bonded methylene hydrogens reveal a shorter distance to the metal ($Zr\cdots H^1_\alpha$ = 2.50 [2.54] Å) and a closer $C_\alpha-Zr-H^1_\alpha$ angle (94.4° [93.3°]) for one of them, while the other H atom shows a longer distance ($Zr\cdots H^2_\alpha$ = 2.90 [2.95] Å) and consequently also a more open $C_\alpha-Zr-H^2_\alpha$ angle (123.2(5)°). The relatively long $Zr\cdots H^1_\alpha$ distance and the observation that both hydrogen atoms are out of the equatorial plane, H^1_α by 0.82(1) [0.87(1)] Å and H^2_α by 0.29(1) [0.32(1)] Å, make a conventional α agostic interaction quite implausible.

The comparable reaction with 1 equiv of (*i*-Pr)MgCl led to a dark-brown solution, from which a mixture of the new alkyl derivative [Zr(CpSi$_2$Cp)Cl(*i*-Pr)], **4**, and the *n*-propyl complex **3** was obtained. When the reaction was monitored by ^{1}H and ^{13}C NMR spectroscopies in a sealed tube, complete transformation of the starting compound **1** into the isopropyl complex **4** was observed. However, at a later stage of the reaction, isomerization takes place with migration of one β-hydrogen from C_β to C_α, presumably through β-hydrogen elimination and reinsertion to give the *n*-propyl complex **3** (Scheme 2).

All of the chloro alkyl complexes were slowly hydrolyzed by the addition of stoichiometric amounts of water in the presence of PMe_3 to afford, in refluxing toluene, the μ-oxo-bridged dimer [{Zr(CpSi$_2$Cp)Cl}$_2$(μ-O)], **5**. When the reactions of **2** and **3** were monitored in sealed NMR tubes by ^{1}H NMR spectroscopy using wet benzene-d_6 (0.014% H_2O), the resulting formation of complex **5** was always accompanied by the dichloro complex **1**. The latter, however, appeared to be a product of the simultaneous thermal decomposition of the alkyl compounds. For this reason, the hydrolysis was carried out in the presence of PMe_3, in order to suppress the decomposition process as discussed below. Complex **5** was isolated as a white solid after recrystallization from toluene and characterized by elemental analysis and NMR spectroscopy (see Experimental Section).

Thermal Decomposition of the Chloro Alkyl Complexes. The decomposition of a THF-d_8 solution of the chloro ethyl complex **2** was studied in a sealed tube by ^{1}H NMR spectroscopy (Scheme 1). A slow transformation was observed at room temperature, which was complete after 1 day, to give the dichloro compound **1**, with evolution of ethane and ethene in a 1:1 molar ratio, leaving an unidentified insoluble residue. This behavior may be explained as a result of the intermediate formation of either the hydride species **A** which then reacts with the chloro ethyl complex evolving C_2H_4 and C_2H_6 or, more likely, the bridged dinuclear species **B** leading to the dichloro and dialkyl complexes, followed by the decomposition of the dialkyl complex by intramolecular β-elimination of C_2H_6 and evolution of C_2H_4. This type of redistribution reaction in polar solvents is well-known for analogous zirconium compounds.[21] Formation of any of these intermediates,

which could not be detected by NMR spectroscopy, should be hindered by the addition of ligands. When the same process was studied in benzene-d_6, formation of the dichloro compound **1** was not observed until the solution was heated to 80 °C. In the presence of PMe_3, the formation of **1** in THF-d_8 was observed to be slower and did not take place at all in benzene-d_6 even after heating for 12 h at 80 °C. A similar behavior was also observed for the *n*-propyl complex.

Synthesis and Thermal Decomposition of the Dialkyl Complexes. The dialkyl complexes [Zr($CpSi_2$-Cp)R_2] (R = Et (**6**), n-Pr (**7**)) were obtained either by reaction of the chloro alkyl derivatives **2** and **3** with 1 equiv of the alkylating agent RMgCl (R = Et, n-Pr) or by the alkylation of complex **1** in THF using an excess amount of RMgCl. When reactions of **1** with excess RMgCl were monitored from −78 to 5 °C by ^{1}H NMR in sealed tubes, a selective total conversion to the chloro alkyl compounds **2** and **3** was observed, which was then followed by further alkylation to give the dialkyl complexes **6** and **7**. After the solution was warmed to −10 (**6**) or −5 °C (**7**), **6** and **7** were identified by ^{1}H and ^{13}C NMR spectroscopies as the only Zr containing components, together with the excess RMgCl (see Experimental Section). Decomposition was observed when the THF-d_8 solution of **6** was warmed to room temperature to give a mixture of the μ-ethene complex [{Zr($CpSi_2$-Cp)Et}$_2$(μ-CH_2=CH_2)], **8**, as the major component and minor amounts of unidentified components. A similar behavior was observed for **7**, which also decomposed at room temperature to yield a mixture of unidentified products. Alkylation of the dichloro complex **1** and the chloro alkyl complexes **2** and **3** was carried out on a preparative scale in THF using stoichiometric amounts of RMgCl (R = Et, n-Pr), which afforded solutions containing the dialkyl compounds **6** and **7**. However, at temperatures higher than 0 °C, the formation of decomposition products could not be avoided so that complexes **6** and **7** could not be isolated in pure form.

A more satisfactory preparation for complex **8** was found to be the reaction of the dichloro complex **1** or the chloro ethyl complex **2** with 2 or 1 equiv of EtMgCl in THF, respectively. Under these conditions, the thermal decomposition of the intermediate diethyl complex **6** was achieved by stirring its THF solution at 0 °C for 3 h. One equivalent of ethane was evolved, and the olefin-bridged dinuclear zirconium complex **8** was formed, which was isolated as orange crystals in 70% yield after recrystallization from diethyl ether. As shown in Scheme 3, either an intra- or intermolecular β-H elimination may be proposed to explain the formation of **8**. Complex **8** is an extremely air sensitive compound for which acceptable analytical values could not be obtained. Examination of its ^{1}H and ^{13}C NMR data shows that all of the ethyl, dimethylsilyl, and cyclopentadienyl ring proton resonances are displaced to higher fields, compared with the corresponding zirconium(IV) alkyl compounds (see Experimental Section). The same behavior was reported[7] for a related methylbis(cyclopentadienyl)zirconium derivative, the only similar compound, whose molecular structure was studied by X-ray diffraction. This might suggest that **8** has to be classified as a zirconium(III) compound. We will return to the problem of the oxidation number of Zr in **8** at a later point in our discussion.

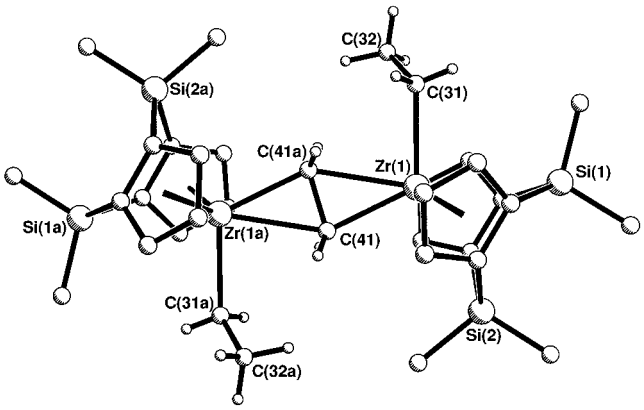

Figure 2. PLUTO view of the molecular structure of [{Zr($CpSi_2Cp$)Et}$_2$(μ-CH_2=CH_2)] (**8**), with the atom numbering scheme.

Scheme 3

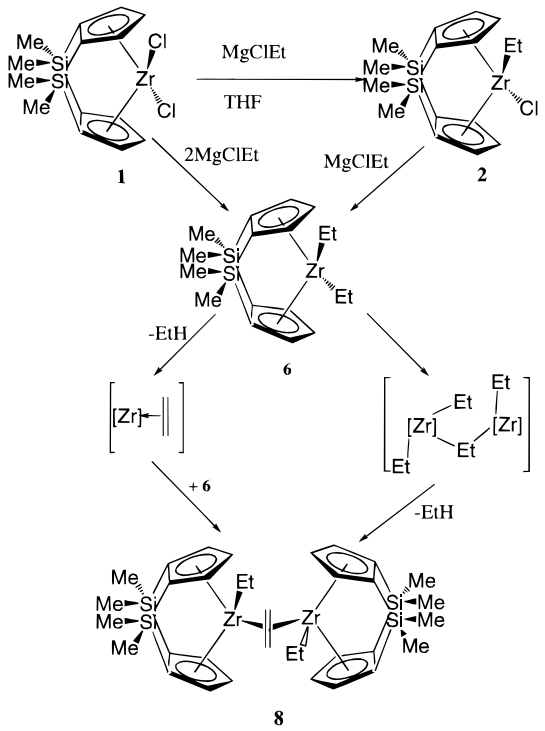

The spectroscopically derived structure of **8** as an olefin-bridged dinuclear species was confirmed by the molecular structure obtained by X-ray crystallography, which is shown in Figure 2. Selected bond angles and distances are given in Table 3. This is the first crystal structure reported for an ethyl ethene zirconium complex.

The molecule can be described as consisting of two di-*ansa*- bis(dimethylsilandiyl)di-η^5-cyclopentadienyl ethyl zirconium fragments bridged by one molecule of ethene. Both zirconium atoms exhibit a pseudotetrahedral coordination if the centroids of the cyclopentadienyl rings, the ethyl α-carbon, and the midpoint of the ethene C−C distance are considered as coordination sites. There are two Cp rings which have the same Zr−C separation (centroid−Zr distances 2.225 and 2.218 Å). From a crystallographic point of view, the molecule is assembled from two moieties related by a center of symmetry located in the middle of the ethene molecule. The methylene carbons of the ethyl group are located practically (0.02 Å) in the equatorial plane. The Zr−

Table 3. Selected Bond Distances (Å) and Angles (deg) for Compound 8[a]

Zr(1)−C(41)	2.306(6)	Zr(1)−C(31)	2.360(6)
Zr(1)−C(22)	2.459(5)	Zr(1)−C(12)	2.464(5)
Zr(1)−C(21)	2.463(5)	Zr(1)−C(11)	2.465(5)
Zr(1)−C(41a)	2.530(5)	Zr(1)−C(25)	2.536(5)
Zr(1)−C(15)	2.549(6)	Zr(1)−C(23)	2.552(5)
Zr(1)−C(13)	2.559(5)	Zr(1)−C(24)	2.599(5)
Si(1)−C(16)	1.858(7)	Si(1)−C(17)	1.865(6)
Si(1)−C(11)	1.875(6)	Si(1)−C(21)	1.882(6)
Si(2)−C(26)	1.865(6)	Si(2)−C(27)	1.869(7)
Si(2)−C(12)	1.874(6)	Si(2)−C(22)	1.877(5)
C(11)−C(15)	1.415(8)	C(11)−C(12)	1.452(8)
C(12)−C(13)	1.415(8)	C(13)−C(14)	1.413(9)
C(14)−C(15)	1.396(8)	C(22)−C(23)	1.410(8)
C(22)−C(21)	1.444(8)	C(24)−C(25)	1.393(8)
C(24)−C(23)	1.410(8)	C(21)−C(25)	1.411(7)
C(31)−C(32)	1.519(9)	C(41)−C(41a)	1.479(12)
Zr(1)−Cp1	2.223	Zr(1)−Cp2	2.217
C(41)−Zr(1)−C(31)	115.6(2)	C(41)−Zr(1)−C(41a)	35.2(3)
C(31)−Zr(1)−C(41a)	80.4(2)	C(16)−Si(1)−C(17)	108.1(3)
C(16)−Si(1)−C(11)	112.2(3)	C(17)−Si(1)−C(11)	116.8(3)
C(16)−Si(1)−C(21)	112.5(3)	C(17)−Si(1)−C(21)	114.3(3)
C(11)−Si(1)−C(21)	92.4(2)	C(26)−Si(2)−C(27)	108.2(3)
C(26)−Si(2)−C(12)	116.1(3)	C(27)−Si(2)−C(12)	112.0(3)
C(26)−Si(2)−C(22)	116.5(3)	C(27)−Si(2)−C(22)	110.6(3)
C(12)−Si(2)−C(22)	92.9(2)	C(15)−C(11)−C(12)	106.9(5)
C(15)−C(11)−Si(1)	125.4(4)	C(12)−C(11)−Si(1)	122.8(4)
Si(1)−C(11)−Zr(1)	96.3(2)	C(13)−C(12)−C(11)	106.7(5)
C(13)−C(12)−Si(2)	126.2(4)	C(11)−C(12)−Si(2)	121.9(4)
C(14)−C(13)−C(12)	109.1(5)	C(15)−C(14)−C(13)	107.9(5)
C(14)−C(15)−C(11)	109.4(5)	C(23)−C(22)−C(21)	106.6(5)
C(23)−C(22)−Si(2)	124.6(4)	C(21)−C(22)−Si(2)	123.7(4)
C(25)−C(24)−C(23)	107.2(5)	C(25)−C(21)−C(22)	106.8(5)
C(25)−C(21)−Si(1)	126.9(4)	C(22)−C(21)−Si(1)	121.1(4)
C(24)−C(25)−C(21)	109.9(5)	C(22)−C(23)−C(24)	109.5(5)
C(41a)−C(41)−Zr(1)	80.7(4)	C(41a)−C(41)−Zr(1a)	64.1(4)
Zr(1)−C(41)−Zr(1a)	144.8(3)	Cp1−Zr(1)−C(41)	107.7
Cp1−Zr(1)−C(41a)	120.3	Cp1−Zr(1)−C(31)	105.3
Cp2−Zr(1)−C(41)	105.4	Cp2−Zr(1)−C(41a)	116.1
Cp2−Zr(1)−C(31)	104.0	Cp1−Zr(1)−Cp2	119.4

[a] Cp1 is the centroid of C(11), C(12), C(13), C(14), and C(15); Cp2 is the centroid of C(21), C(22), C(23), C(24), and C(25).

ethyl bond distance of 2.357(6) Å corresponds to a single bond. The $Me-C_2H_5$ group points toward one of the cyclopentadienyl rings. Thus, the $Zr-C_\alpha-C_\beta$ plane forms a dihedral angle of 59.8(4)° with the equatorial plane. The C_β atom is displaced 1.083(8) Å from the equatorial plane. The ethene carbon atoms are located almost in the equatorial plane (defined by the Si and Zr atoms) and are bonded to the Zr atoms in an asymmetric fashion, with Zr−C(41) and Zr−C(41A) bond distances of 2.304(5) and 2.531(6) Å, respectively. The olefinic C−C bond length is elongated to 1.48(1) Å. A single-bond distance (1.518(9) Å) is observed for the C−C bond of the ethyl group. The four hydrogens of the ethene molecule are alternately displaced from the molecular plane of the free olefin, away from the less distant zirconium center.

Extending the comparison of **8** with **2**, further similarities are observed in the zirconium−carbon ring distortions. The internal bridgehead carbon atoms are located at distances ca. 0.1 Å shorter than the external ones, and again, the bending angle θ between the two cyclopentadienyl rings of 119.4° is very narrow.

Theoretical Studies. We performed DFT calculations on the molecule $[\{ZrCp_2Me\}_2(\mu\text{-}CH_2{=}CH_2)]$, **8a**, which serves as a model complex for compound **8**. The geometry of the methyl and cyclopentadienyl ligands was fixed (see Computational Details), and C_i symmetry was employed, according to the symmetry of **8** in the crystal. The starting point of our optimization was a structure with a symmetrically bonded μ-C_2H_4 ligand. This arrangement converged into an asymmetric coordination geometry of the bridging ethene. Its structure is shown in Chart 1, together with selected experimental and calculated bond distances.

Chart 1

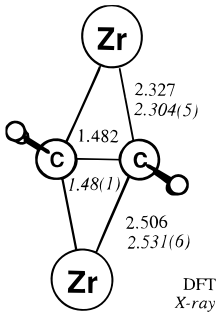

0 kJ/mol

Chart 2

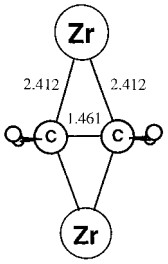

19 kJ/mol

The calculated geometry matches the X-ray structure with satisfactory agreement. The elongated C−C bond is represented exactly within the experimental error, and the calculated Zr−C distances deviate by 0.02−0.03 Å. Furthermore, the C_2H_4 moiety adopts the trans bent distorted coordination geometry, as found in the crystal structure. The fold angle of the CH_2 unit amounts to 42°, some 6° smaller than the experimental value. Takahashi and co-workers[7] report for $[\{ZrCp_2Me\}_2(\mu\text{-}CH_2{=}CH_2)]$ the following geometry of the C_2H_4 ligand: two distinctly different Zr−C distances of 2.327(6) and 2.528(4) Å and a C−C separation of 1.473(7) Å. They also found the ethylene unit to posses a trans bent distorted geometry. The coordination mode of C_2H_4 in Takahashi's molecule is identical to that observed for compound **8**, and the geometric parameters are very similar to those found for **8**, as well as those calculated for **8a** (compare to Chart 1).

Enforcing a planar geometry of the coordinated C_2H_4 ligand resulted in $[\{ZrCp_2Me\}_2(\mu\text{-}CH_2{=}CH_2)_{planar}]$, **8b**, whose structure is shown in Chart 2. Here, we find the ethene coordinating to the two zirconium centers in a symmetrical fashion with two equal Zr−C distances. The Zr−C separation amounts to 2.412 Å, which is roughly the mean value of the two Zr−C distances as found in **8** or **8a**. The C−C distance in **8b** is about 0.002 Å shorter than the one in **8a**. However, the structure with ethene coordinated in a planar fashion is 19 kJ/mol higher in energy than the trans bent distorted geometry.

We now want to analyze how the trans bent distortion might stabilize the coordination of C_2H_4, sandwiched between two $ZrRCp_2$ fragments. We begin with a brief

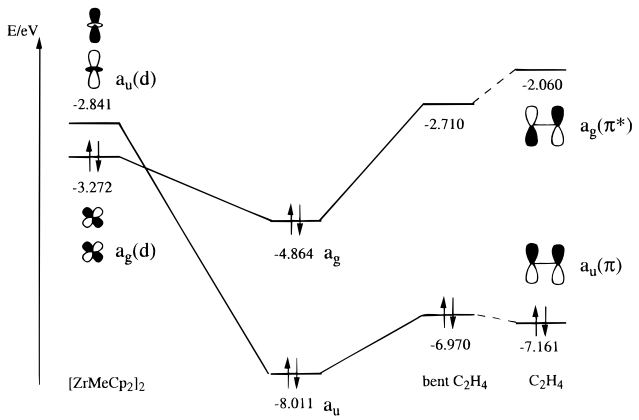

Figure 3. Orbital interaction diagram for the formation of [ZrCp$_2$Me]$_2$(μ-CH$_2$=CH$_2$) (**8a**) from the fragments {ZrCp$_2$Me}$_2$ and CH$_2$=CH$_2$.

look at the ZrCp$_2$ fragment as the basic element. The classic work by Lauher and Hoffmann[22] and Brintzinger[23] and co-workers provides the essential orbital analysis for MCp$_2$ fragments, from which a great deal of the chemistry of transition metal biscyclopentadienyl complexes can be understood on qualitative grounds. Lauher and Hoffmann identify three orbitals as being crucial in determining the structure of MCp$_2$ complexes. They are termed—according to C_{2v} symmetry and in order of increasing energy—1a$_1$, 1b$_2$, and 2a$_1$. Theses orbitals are all located in the equatorial plane, which is the plane containing the metal center and perpendicular to that defined by the metal center and the centroids of the two Cp rings. It is important to note that these three orbitals drop in energy when the bending angle of the MCp$_2$ moiety is increased. Recently, Bürgi et al. analyzed the influence of the bent angle on the reactivity and coordination chemistry of ZrCp$_2$ complexes.[24]

We proceed with a fragment analysis of the interaction of C$_2$H$_4$ with the bimetallic fragment, to give compound **8** (eq 1). The orbital interaction diagram for

$$\{ZrCp_2Me\}_2 + CH_2{=}CH_2 \rightarrow \{ZrCp_2Me\}_2(\mu\text{-}CH_2{=}CH_2) \quad (1)$$

this process is shown in Figure 3. On the left hand side of Figure 3, we find the HOMO, a$_g$(d), and LUMO, a$_u$(d), of the {ZrCp$_2$Me}$_2$ fragment. The prominent contributions to these orbitals are antisymmetric combinations of the 1b$_2$ and the 2a$_1$ orbitals of the two ZrCp$_2$ moieties, respectively. On the right hand side, we see the corresponding ethene orbitals, namely a$_u$(π) and a$_g$(π*). The two sets of fragment orbitals combine with the molecular orbitals a$_g$, representing donation from the π orbital of ligand to the metal centers, and a$_u$, the HOMO of **8a** characterizing the back-donation into the π* orbital of the ligand.

The trans bent distortion of C$_2$H$_4$ significantly destabilizes the C−C double bond, and as a consequence, the a$_u$(π) orbital rises in energy by 0.191 eV, whereas a$_g$-(π*) significantly drops in energy by 0.650 eV (Figure 3). In this way, both ligand orbitals come closer in energy to their metal-based counterparts. Thus, the trans bent distortion leads to a better energetic match of the interacting orbitals, which in turn enhances the bond strength between the two combining fragments.

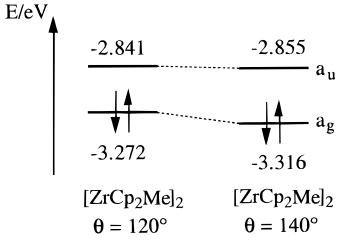

Figure 4. The frontier orbitals of the [ZrCp$_2$Me]$_2$ fragment drop in energy when the bite angle θ increases.

Having understood the effect of the trans bent distortion of C$_2$H$_4$, we now want to analyze the role of the narrow bending angle of the zirconocene fragments. To this end, we performed calculations on a hypothetical molecule with a rather open bending angle of 140°, [{ZrCp$_2$Me}$_2$(μ-CH$_2$=CH$_2$)$_{\theta=140°}$], **8c**. The geometry of the coordinated CH$_2$=CH$_2$ varies only slightly compared to that of **8a** (d_{C-C} = 1.479, $d1_{Zr-C}$ = 2.332 Å, $d2_{Zr-C}$ = 2.500 Å). The way the frontier orbitals of the {ZrCp$_2$-Me}$_2$ fragment change under this distortion is however of interest. As mentioned before, the 1b$_2$ and the 2a$_1$ orbitals of the ZrCp$_2$ fragment drop in energy when the bent angle is increased. Since the frontier orbitals a$_g$-(d) and a$_u$(d) are dominated by contributions from 1b$_2$ and 2a$_1$, we can expect the same trend here. This is indeed the case; opening the bent angle by 20° stabilizes a$_g$(d) and a$_u$(d) by 0.044 and 0.014 eV, respectively (Figure 4). According to Figure 3, this change would enhance the π donation from, but also diminish the π* back-donation to, the C$_2$H$_4$ ligand. We further note that these shifts in energy are rather subtle compared to those occurring under trans bent distortion. It is no longer obvious what the net result of the change in the bent angle would be on the bond strength of the ethene ligand.

To get a better understanding of this problem, we performed a detailed bonding anlysis[25] of the interaction between {ZrCp$_2$Me}$_2$ and CH$_2$=CH$_2$. The change in energy associated with the reaction as formulated in eq 1, the so-called bond snapping energy BE_{snap}, can be written as with ΔE^0 as the steric repulsion term and

$$BE_{snap} = -[\Delta E^0 + \Delta E_{int}(a_g) + \Delta E_{int}(a_u)] \quad (2)$$

$\Delta E_{int}(a_g)$ and $\Delta E_{int}(a_u)$ as the orbital interaction terms. ΔE^0 is dominated by Pauli repulsion and is usually and in all of our cases, repulsive. The terms $\Delta E_{int}(a_g)$ and $\Delta E_{int}(a_u)$ introduce an attractive bonding interaction and describe π* back-donation and π donation, respectively. Finally, we obtain the bonding energy BE by taking into account the preparation energy ΔE_{prep} (eq 3). ΔE_{prep} is

$$BE = BE_{snap} - \Delta E_{prep} \quad (3)$$

the energy that is required to make the fragments ready for a bonding interaction. In our case, it essentially describes the deformation energy of the ethene ligand

(22) Lauher, J. W.; Hoffmann R. *J. Am. Chem. Soc.* **1976**, *98*, 1729.
(23) (a) Brintzinger, H. H. Bartell, L. S. *J. Am. Chem. Soc.* **1970**, *92*, 1105. (b) Brintzinger, H. H.; Lohr, L. L., Jr.; Wong, K. L. T. *J. Am. Chem. Soc.* **1975**, *97*, 5146.
(24) Bürgi, T.; Berke, H.; Wingbermühle, D.; Psiorz, C; Noe, R.; Fox, T.; Knickmeier, M.; Berlekamp, M.; Fröhlich, R.; Erker, G. *J. Organomet. Chem.* **1995**, *497*, 149.
(25) (a) Baerends, E. J.; Rozendaal, N. *NATO ASI Ser.* **1986**, *C176*, 159. (b) Ziegler, T. *NATO ASI Ser.* **1991**, *C378*, 367.

Table 4. Energy Decomposition[a] for the Reaction $\{ZrCp_2Me\}_2 + CH_2{=}CH_2 \rightarrow \{ZrCp_2Me\}_2(\mu\text{-}CH_2{=}CH_2)$ for the Complexes 8a−c

	8a (C_2H_4) bent $\theta = 120°$	**8b** (C_2H_4) planar $\theta = 120°$	**8c** (C_2H_4) bent $\theta = 140°$
ΔE^0	720	741	817
$\Delta E_{int}(a_g)$	−917	−872	−906
$\Delta E_{int}(a_u)$	−155	−151	−180
BE_{snap}	352	282	269
ΔE_{prep}	89	38	89
BE	263	244	180

[a] In kJ/mol.

from its equilibrium geometry to the final framework of the molecule.

The results of these analyses for the molecules **8a−c** are collected in Table 4. We begin with a short look at **8a**, our model system for the "real life" complex **8**. When the two contributions to the orbital interaction are compared, it is evident that $\Delta E_{int}(a_g)$ is about six times higher than $\Delta E_{int}(a_u)$. Thus, the bonding in **8** is mainly determined by π^* back-donation to the ethene ligand, and the contribution due to π donation only plays a minor role. When going from **8a** to **8b**, the complex with a planar coordinated ethene, we observe a drop in both of the contributions to the orbital interaction energy. This is in accord with the trend, as predicted above. We also observe an increase in the repulsive steric interaction energy. The C_2H_4 coordination mode in **8b** is less favorable to that in **8a** with respect to both electronic as well as steric effects. However, **8b** requires only half the amount of preparation energy compared to **8a**, and both structures differ in energy by only 19 kJ/mol. Opening the bent angle, **8c**, indeed leads to an increase in π donation, as well as to a decrease in π^* back-donation. Yet in terms of the overall orbital interaction, **8c** is favored over **8a** by 14 kJ/mol. It is the large increase in steric repulsion which makes **8a** the energetically preferred structure. The role of the narrow bent angle in the zirconocene fragments is not that of enhancing orbital interaction, but rather that of reducing steric repulsion.

Lastly, we return to the problem of the oxidation number of Zr in complex **8**. The key point in this question is whether the C_2H_4 bridging unit has to be regarded as $H_2C{=}CH_2$ or $[H_2C{-}CH_2]^{2-}$. Mulliken atomic charges might help to solve the problem. For the free ligand, we calculated the gross atomic charge at carbon, AC_C, to amount to −0.045 au. This value increases up to −0.715 au when the C_2H_4 ligand is brought into the coordination sphere of complex **8a**. In comparison, for the system $Cp_2Zr(H_2C{=}CH_2)$, we find an AC_C of only −0.221 au. The large charge flow to the ethene carbons is consistent with the fact that back-donation into the π^* orbital of ethene contributes the major bonding interaction. The strong population of this antibonding orbital formally reduces the C−C bond order from two to one, a fact which manifests itself also in the very long C−C bond. This all suggests that the bridging unit in **8** should be described as $[H_2C{-}CH_2]^{2-}$ and that the metal centers in **8** should be regarded as Zr(IV).

Conclusions

The first β hydrogen containing alkyls, the ethyl and *n*-propyl derivatives of the di-*ansa*-bis(dimethylsilanediyl)dicyclopentadienyl zirconium dichloride [$Zr(CpSi_2Cp)Cl_2$], have been isolated and structurally characterized. The monoalkylated compounds are thermally stable up to 10 °C but decompose at higher temperatures through an intermolecular reaction to give [$Zr(CpSi_2Cp)Cl_2$] and an equimolar mixture of alkane and alkene. This decomposition is favored in polar solvents and prevented by addition of PMe_3. However, the dialkylated compounds could not be isolated as solids as they decompose with evolution of alkane. From this decomposition, a new μ-ethene dinuclear zirconium ethyl complex was isolated in 70% yield and was studied by X-ray diffraction. The molecular structures of the chloro ethyl and the μ-ethene zirconium ethyl complexes show very close bending angles of 120.6° and 119.8°, respectively.

Acknowledgment. Support from DGICYT (Project PB-92-0178-C) and the Swiss National Science Foundation (SNSF) is gratefully acknowledged. F.J.F. and A.M. acknowledge MEC-FPI and CAM for the award of fellowships. We thank the Rechenzentrum der Universität Zürich for providing access to their computing facilities.

Supporting Information Available: Tables of atomic coordinates and equivalent isotropic displacement parameters (Table 1S), anisotropic displacement parameters (Table 2S), and hydrogen coordinates and isotropic displacement parameters (Table 3S) for compound **8** and positional parameters and estimated standard deviations (Table 4S), hydrogen positional parameters and estimated standard deviations (Table 5S), and general displacement parameters (Table 6S) for compound **2** (10 pages). Ordering information is given on any current masthead page.

OM9610509